Advanced Two-Moment Bulk Microphysics for Global Models. Part I: Off-Line Tests and Comparison with Other Schemes

A. GETTELMAN AND H. MORRISON

National Center for Atmospheric Research, Boulder, Colorado*

(Manuscript received 31 January 2014, in final form 29 August 2014)

ABSTRACT

Prognostic precipitation is added to a cloud microphysical scheme for global climate models. Results indicate very similar performance to other commonly used mesoscale schemes in an offline driver for idealized warm rain cases, better than the previous version of the global model microphysics scheme with diagnostic precipitation. In the mixed phase regime, there is significantly more water and less ice, which may address a common bias seen with the scheme in climate simulations in the Arctic. For steady forcing cases, the scheme has limited sensitivity to time step out to the ~15-min time steps typical of global models. The scheme is similar to other schemes with moderate sensitivity to vertical resolution. The limited time step sensitivity bodes well for use of the scheme in multiscale models from the mesoscale to the large scale. The scheme is sensitive to idealized perturbations of cloud drop and crystal number. Precipitation decreases and condensate increases with increasing drop number, indicating substantial decreases in precipitation efficiency. The sensitivity is less than with the previous version of the scheme for low drop number concentrations ($N_c < 100\,\mathrm{cm}^{-3}$). Ice condensate increases with ice number, with large decreases in liquid condensate as well for a mixed phase case. As expected with prognostic precipitation, accretion is stronger than with diagnostic precipitation and the accretion to autoconversion ratio increases faster with liquid water path (LWP), in better agreement with idealized models and earlier studies than the previous version.

1. Introduction

Advances in computational power have led to the ability to increase complexity in atmospheric models at all scales, from large-eddy simulations (LES) to global general circulation models (GCMs) used for weather and climate prediction. Central to high-resolution modeling of weather and climate is the evolution of condensed water and ice in clouds, which determines the evolution of latent heating, precipitation, and the radiative balance of the planet. Because these processes occur on small scales they are typically parameterized as cloud "microphysics," that is, the physical processes with a typical scale of cloud droplets (10^{-6} m). Recent advances in global simulation of cloud microphysics have led to adoption of many characteristics of relatively sophisticated microphysical schemes designed for small-scale limited area models. This includes explicit representation of cloud drop and crystal size distributions using prognostic moments (e.g., Morrison and Gettelman 2008, hereafter MG2008), and links between number concentration of cloud drops and aerosols based on empirical correlations (Boucher and Lohmann 1995) or physical treatments (Abdul-Razzak and Ghan 2000).

However, many or most global models still have simplified treatments of microphysics in convective clouds, which has only recently been addressed (Song et al. 2012; Lohmann 2008). The MG2008 scheme has been modified by Song et al. (2012) to apply inside of deep convective clouds and, with the configurations of Bogenschutz et al. (2012), it has also been applied to shallow convective regimes. Most large-scale (stratiform) microphysical schemes are still operating over relatively long (10–30 min) time steps, which may induce numerical problems. Schemes also typically assume diagnostic precipitation, meaning that the precipitation

Denotes Open Access content.

* The National Center for Atmospheric Research is sponsored by the National Science Foundation.

Corresponding author address: A. Gettelman, National Center for Atmospheric Research, 1850 Table Mesa Dr., Boulder, CO 80305.
E-mail: andrew@ucar.edu

DOI: 10.1175/JCLI-D-14-00102.1

mass in the atmosphere is rediagnosed each time step based on a steady-state assumption of the precipitation source and sink terms. Prognosing precipitation across time steps has been shown to significantly alter the evolution of clouds and precipitation (Posselt and Lohmann 2009). This arises largely because the balance of rain formation processes (particularly the collection of cloud drops by rain, or accretion) is dependent on the existence of rain, and the microphysical sources and sinks are sensitive to this process (Gettelman et al. 2013). Recent studies have provided evidence that diagnostic precipitation may lead to biases in process rate calculations (Posselt and Lohmann 2008; Wang et al. 2012; Gettelman et al. 2013). These studies hint that a better representation of the microphysics of precipitation is important for properly representing precipitation and cloud lifetime, and also show that prognostic precipitation (carried across time steps) alters the behavior of accretion. The precipitation process has been shown to be sensitive to drop number (and hence the population of aerosols that affect drop number) in idealized models (Wood et al. 2009), large-eddy simulation experiments (Jiang et al. 2010), and analysis of observations (Terai et al. 2012).

While most GCM microphysics schemes calculate precipitation diagnostically, a few have been developed for climate modeling that prognose precipitation. For example, Fowler et al. (1996) introduced a one-moment bulk scheme predicting mass mixing ratios of cloud water, cloud ice, snow, and rain into the Colorado State University GCM and found good agreement with observations in terms of water paths, cloudiness, and cloud radiative forcing; they also noted the importance of interactions between the cloud microphysics and cumulus convection parameterizations on surface precipitation. Lopez (2002) introduced prognostic equations for the rain and snow mass mixing ratios into the Action de Recherche Petite Echelle Grande Echelle (ARPEGE) global spectral model and found good performance relative to observations for both higher-resolution numerical weather prediction (NWP) and coarser-resolution climate simulations. Posselt and Lohmann (2008) introduced prognostic equations for rain mass mixing ratio and number concentration (i.e., a two-moment approach) with the goal of improving warm rain microphysical process rates and cloud–aerosol interactions. They found that the introduction of prognostic rain led to a change in the relative balance of autoconversion and accretion, which led to a substantial reduction in the magnitude of radiative forcing from aerosol indirect effects. All three studies noted sensitivity to the time step, which is an important issue because of the long time steps in GCMs. Prognostic precipitation and substepping microphysics has also recently been implemented in the Met Office (UKMO) model by Walters et al. (2014); they found that it improved the light rain regime.

In this paper and its companion, we will present an update to the MG2008 microphysics scheme, and describe the implementation in the Community Atmosphere Model (CAM). In this work the diagnostic treatment of rain and snow mass and number mixing ratios is replaced with a prognostic treatment. The main unique aspect relative to the other schemes developed for GCMs with prognostic precipitation noted above is the prognostic two-moment approach for *all* hydrometeor categories, including cloud liquid water (suspended liquid) and cloud ice (suspended ice) as well as rain (large size falling liquid) and snow (large size falling ice). Thus, the updated scheme is conceptually similar to fully two-moment schemes that have been developed for higher-resolution cloud and mesoscale models and applied to all cloud types (not just stratiform clouds). The main drawback for using this new scheme in deep convection is the lack of representation of dense rimed ice (graupel/hail). Given this conceptual similarity we compare the updated scheme with two other widely used schemes previously developed for higher-resolution models. This is done in an idealized framework with specified dynamics to allow a direct comparison of the schemes. We also test sensitivity of these schemes over a wide range of time steps and vertical grid spacings, from values for cloud models to GCMs.

Part I (the present paper) describes the updates to the scheme and makes comparisons with the other schemes and numerical tests, and Gettelman et al. (2014, hereafter Part II) will show single-column and global results. Part I is organized as follows. Section 2 describes the scheme. Section 3 introduces the offline model configuration. Basic results and comparisons with other schemes are in section 4, and detailed sensitivity tests looking at process rates are in section 5. Conclusions are in section 6.

2. Scheme description

The two-moment scheme described by MG2008 and Gettelman et al. (2010) (hereafter this scheme is referred to as MG1) has been slightly modified with small feature fixes, and a refactoring of the code. Updating the prognostic droplet number mixing ratio (in kg^{-1}) with the tendency from droplet activation has been moved to the beginning of the scheme, for consistency with updating cloud liquid mass with condensation/evaporation tendencies before the microphysical process calculations. This version of the code is a control case, and we

call it MG1.5. The only significant change in simulated climate between MG1 and MG1.5 is from the modification of when the droplet activation tendency is applied. The major focus of this work is to extend MG1.5 to include prognostic precipitation (hereafter MG2). The base MG1.5 scheme includes prognostic variables for cloud water and ice mass and number mixing ratios and calculates rain and snow mass and number mixing ratios (q_r, q_s, N_r, and N_s) diagnostically. Microphysics schemes in GCMs have traditionally employed diagnostic precipitation [with some notable exceptions such as in Posselt and Lohmann (2008)] because (i) for long time steps it avoids problems of violating the Courant–Fredrichs–Levy (CFL) stability conditions for sedimentation of precipitation, (ii) there is reduced computational cost of not having to advect additional precipitation variables, and (iii) the large grid spacing implies that horizontal advection of precipitation is unimportant. Assuming a $10\,\mathrm{m\,s^{-1}}$ horizontal wind speed and a residence time of 10–60 min for rain and snow with a fall speed of $1–5\,\mathrm{m\,s^{-1}}$ falling 5 km implies that advection of precipitation is important for grid spacings smaller than ~10–50 km. However, because of the long residence time of precipitation in the atmosphere relative to even GCM time steps, especially for snow, the diagnostic treatment may lead to inconsistencies because it assumes precipitation evaporates or falls to the surface within the time step. Moreover, numerically solving the diagnostic precipitation equations is highly challenging (discussed below), which can lead to errors even when the diagnostic steady-state assumption is reasonable (i.e., for long time steps and coarse spatial resolutions). Thus, the use of diagnostic precipitation can lead to biases in process rates such as accretion that depend on the precipitation mass in the atmosphere (Gettelman et al. 2013).

The diagnostic treatment of precipitation means that rain and snow in the atmosphere is not tracked across time steps. Instead q_r, q_s, N_r, and N_s are calculated assuming time tendencies are zero. This results in a set of coupled ordinary differential equations for q_r, q_s, N_r, and N_s that depend only on height z [see Eqs. (11) and (12) in MG2008] and are therefore solved by vertical integration from cloud top downward. Because the source/sink terms for precipitation depend on q_r, q_s, N_r, and N_s, especially for accretion processes (collection of cloud water by rain and snow), simple approaches such as the forward-Euler method produce large errors. Various approaches have been proposed for this integration (Ghan and Easter 1992; MG2008). Ghan and Easter (1992) used the precipitation mass mixing ratios from the previous model time step to estimate the source/sink terms and precipitation mass mixing ratios at the updated time level. In MG1 this integration was done by discretizing and numerically integrating downward using an iterative predictor/corrector-type approach to estimate the source/sink terms and q_r, q_s, N_r, and N_s. Specifically, provisional values of q_r, q_s, N_r, and N_s at a vertical level k were estimated based on the autoconversion rate calculated at the k level (which does not depend on q_r, q_s, N_r, or N_s) combined with the flux of rain from the $k-1$ level above and all other source/sink terms except autoconversion at the $k-1$ level. These provisional values were then used to estimate source/sink terms at the k level, with these source/sink terms subsequently used to calculate final estimates of q_r, q_s, N_r, and N_s (see MG08 for details).

This approach to precipitation has been modified in MG1.5 to use a midpoint type method. In this newer approach the flux of precipitation mass and number from above and the source/sink term at the $k-1$ level (except for autoconversion, for which the values at the k level are again used) are used to estimate q_r, q_s, N_r, and N_s at the $k-1/2$ level. The q_r, q_s, N_r, and N_s at the $k-1/2$ level are then used to calculate the source/sink terms at the $k-1/2$ level, which are then applied to calculate q_r, q_s, N_r, and N_s at the k level. We have verified that the two methods (used in MG1 and MG1.5) do not produce significant differences in climate simulations.

A primary challenge of diagnostic precipitation is that there are sharp vertical gradients in cloud quantities, especially near cloud top. This presents difficulties for numerical integration from cloud top downward required to solve the diagnostic precipitation equations, motivating the implementation of various numerical methods as described above. Nonetheless uncertainties remain, especially because of the coarse vertical grid spacing in typical GCMs, combined with long time steps and complicated interlinkages with the prognostic equations for the cloud water and ice mass and number mixing ratios (q_c, q_i, N_c, and N_i).

For MG2, the MG1.5 scheme is modified by retaining time tendencies for precipitation quantities and solving the following conservation equations:

$$\frac{\partial q_x}{\partial t} = -\frac{1}{\rho}\nabla\cdot(\rho\mathbf{u}q_x) - \frac{1}{\rho}\frac{\partial(\rho V_{q_x} q_x)}{\partial z} + S_{q_x} \quad \text{and} \tag{1}$$

$$\frac{\partial N_x}{\partial t} = -\frac{1}{\rho}\nabla\cdot(\rho\mathbf{u}N_x) - \frac{1}{\rho}\frac{\partial(\rho V_{N_x} N_x)}{\partial z} + S_{N_x}, \tag{2}$$

where the subscript x is either r (rain) or s (snow), t is time, ρ is air density, $\mathbf{u}$ is the 3D wind vector, and V_{q_x} and V_{N_x} are the mass- and number-weighted particle fall speeds. Here S_{q_x} and S_{N_x} are source/sink terms for the mass and number mixing ratios that include the

microphysical process calculations. All microphysical process rate formulations follow MG2008, except that evaporation of rain number mixing ratio is treated by assuming the change in number is proportional to the change in mass during evaporation (analogous to assuming no change in mean raindrop size from evaporation) following Khairoutdinov and Kogan (2000). MG1 neglected the reduction of rain number mixing ratio during evaporation. The impact of this change primarily alters rain mass and number, as discussed below. As in MG1, we do not consider turbulent diffusion of precipitation.

In MG2, Eqs. (1) and (2) are solved together with the conservation equations for q_c, q_i, N_c, and N_i [see Eqs. (6) and (7) in MG2008]. Following MG1 and MG1.5, all microphysical process rates except sedimentation, cloud ice melting, and homogeneous freezing of cloud water are calculated from the prognostic variables updated after applying tendencies from droplet activation, cloud macrophysics (cloud water condensation and evaporation), shallow and deep convection, boundary layer turbulent mixing, and grid-scale advection over the time step. These microphysical processes (except for the three mentioned above) are calculated from the same state and then added together (process split). Checks are made to ensure conservation of all microphysical prognostic variables, and process rates are reduced based upon the available mass for a given species at a rate linearly proportional to the unscaled process rates so that tendencies cannot result in negative mass or number for each hydrometeor category or water vapor. The prognostic variables are then updated, followed by calculation of sedimentation for all prognostic cloud and precipitation variables in MG2 using the first-order upwind method (substepped as needed for numerical stability so that CFL < 1 for the largest mass-weighted fall speed in the vertical column), as employed in many other microphysics schemes. This method is also used to calculate sedimentation of the prognostic cloud variables in MG1 and M1.5, but sedimentation of precipitation is treated diagnostically as described above. This is a key difference between MG2 and the earlier versions of MG. In all versions of MG, melting of cloud ice, homogeneous freezing of cloud water, and saturation adjustment (to condense any excess supersaturation with respect to liquid water generated by the microphysical process rates) are calculated after sedimentation. This is done because these are considered ''fast'' processes and this limits excessive liquid water colder than the homogeneous freezing threshold (−40°C).

The code has several additions that we will take advantage of for testing. All versions of MG have the functionality to work with partially cloudy grid boxes and include an assumed subgrid variance of cloud water. The effect of the subgrid assumption is analyzed in Gettelman et al. (2008) and Lebsock et al. (2013). For MG1.5 and MG2, we now allow the code to be switched to work with uniform grid box properties (no subgrid variability of cloud water, and binary cloud fractions of either 0 or 1). All simulations in this paper assume uniform properties in the grid box. This facilitates testing of the code, and makes it testable against other schemes developed for mesoscale models that assume uniform grid box properties. To facilitate testing we have also enabled the code to use a fixed drop and/or ice crystal number. In addition, we have altered how the code can be substepped to enable better and more flexible coupling with the large-scale condensation (cloud macrophysics). The substepping and coupling is not used here (except substepping of sedimentation for prognostic precipitation in MG2 as described above) but is described in more detail in Part II.

3. Methods

To isolate and test the microphysics we use a simple offline driver with a prescribed one-dimensional flow, the Kinematic Driver (KiD), described by Shipway and Hill (2012). KiD provides a one-dimensional (1D) idealized framework in which to test and compare microphysics schemes. We use simple 1D cases with idealized conditions, driven by an imposed updraft or condensation rate. KiD provides a flexible framework to test different microphysical schemes. It also enables us to test at fine resolution (25-m vertical resolution and 1-s time steps), as well as scale this back to typical GCM resolutions (500-m vertical and 15-min time steps).

KiD predicts potential temperature, water vapor mixing ratio, hydrometeors, and aerosols. For these cases we ignore the effect of aerosols and fix the drop and ice crystal number used in the microphysics. We include sensitivity tests which vary the fixed cloud droplet and ice numbers. KiD uses a 1D monotonic advection scheme, the total variance diminishing (TVD) scheme of Leonard et al. (1992).

We focus on several warm rain cases, with one mixed phase and one cirrus (pure ice) case. A basic warm rain case (Warm 1 or W1) has a single time dependent updraft peaking at 2 m s^{-1} (Table 1). We also explore warm rain cases with oscillating updrafts (W2, W3, and W7) and an oscillating updraft case at cold temperatures that generates a mixed phase cloud (Mixed 3: M3). We also construct a case of a pure ice cloud (Ice 1: I1) with a 12-km top, 100-m vertical grid spacing, and a moist layer from 6 to 12 km. The notation follows the cases described in the KiD distribution (http://appconv.metoffice.com/microphysics) to facilitate comparison

TABLE 1. Description of KiD cases.

Case	Max updraft ($m\,s^{-1}$)	Type	Time (h)	Height (km)	Description
Warm 0 (W0)	none	Steady	8	3	Forced condensation: $5 \times 10^{-7}\,kg\,kg^{-1}\,s^{-1}$
Warm 1 (W1)	2	Evolving	1	3	Single sinusoidal updraft of 600 s
Warm 2 (W2)	2	Evolving	2	3	Multiple sinusoidal updrafts of 600 s
Warm 3 (W3)	2	Evolving	1	3	Multiple updrafts that get weaker over time
Warm 7 (W7)	0.5	Evolving	8	3	Oscillating (600 s) updraft 0–400 m
Mixed 3 (M3)	0.1	Evolving	6	3	Oscillating (600 s) updraft 0–400 m, $T < 0°C$
Ice 1 (I1)	2	Evolving	2	12	1 sinusoidal 1600-s updraft, moist layer 6–10 km

with other work. We also present an idealized case with a directly forced condensation rate (W0) of $5 \times 10^{-7}\,kg\,kg^{-1}\,s^{-1}$, designed to test the numerics of the microphysical scheme. Because the GCM forcing is steady (constant condensation) over long time steps, the W0 case is more similar to the GCM; it ensures that the condensation rate is constant regardless of time step, whereas a standard simulation of KiD will have a variable condensation rate. Condensation serves as a forcing for the microphysics, so we wish to keep this constant to evaluate the time step sensitivity of the microphysics itself. In W0 the vertical velocity is zero, so there is no vertical advection, and the only vertical transport is from the sedimentation calculated by the microphysics. The details of these cases are illustrated in Table 1.

We will also compare MG1.5 and MG2 to two other commonly used microphysics schemes for mesoscale models. These schemes are also run in KiD. The scheme of Morrison et al. (2005) (hereafter this scheme is called M2005) is the predecessor to MG1.5 and MG2 described here. Morrison et al. (2009) further detail the version of the M2005 code with graupel/hail implemented in KiD. Like MG1.5, M2005 is also a two-moment scheme. The major differences between MG1.5 (and MG1) and M2005 lie in diagnostic versus prognostic treatments of precipitation, different aerosol activation, explicit treatment of subgrid variability in MG, representation of ice phase processes, and a dense rimed ice hydrometeor category (graupel or hail) in M2005. Using settings for (i) fixed drop number, (ii) no subgrid variability, and (iii) prognostic precipitation, the MG2 scheme is scientifically identical to M2005 for warm rain cases, but with a very different code development path. We will evaluate the differences below. The Thompson et al. (2008) scheme, modified with the addition of prognostic rain and placed into KiD identified as T2009 (the name of the modified Thompson scheme), has representations of liquid, ice, rain, snow, and graupel, and includes two-moments for cloud ice and rain. It includes several other differences from M2005 including different formulations for several microphysical processes and a nonspherical shape for snow particles.

KiD is run with a 1-s time step and 120 levels in the vertical, with vertical resolution of 25 m (100 m for the I1 case) and fixed cloud droplet number concentrations in all schemes and fixed ice crystal number concentration in MG1.5 and MG2. M2005 and T2009 calculate ice nucleation as a function of temperature following Cooper (1986). We alter these assumptions in several ways to test the microphysics. One of the biggest constraints on time step stability is the numerical stability of the model with respect to advection from air motion, represented by the CFL criterion ($C = u\Delta t/\Delta x$, with instability for $C > 1$). Because the GCM runs with long (10–30 min) time steps and lower vertical resolution, we lower the number of vertical levels to 6, resulting in vertical grid spacing (dz) in the W1 case increasing from 25 to 500 m. As illustrated in Fig. 1 this substantially increases the range over which the CFL condition for numerical stability with respect to the $2\,m\,s^{-1}$ updraft has $C < 1$, from 8 to over 200 s. Note that there is a separate stability criterion for sedimentation of hydrometeors since this is calculated separately from advection due to air motion. Numerical stability for sedimentation in all of the schemes tested here is ensured by substepping as needed, as described above. We

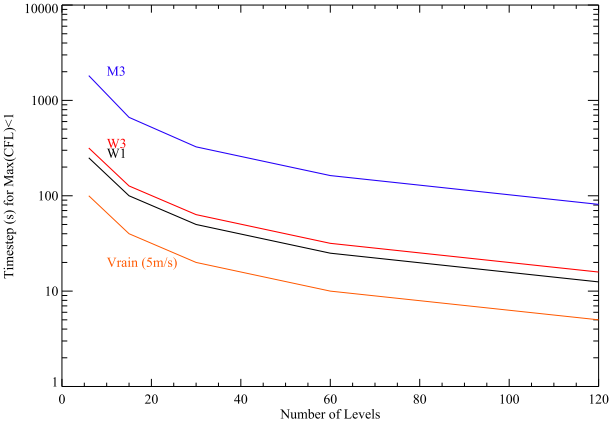

FIG. 1. Maximum time step for maintaining CFL < 1 for cases Warm 1 (W1), Warm 3 (W3), and Mixed 3 (M3) and for a fall speed for rain (V_{rain}) of $5\,m\,s^{-1}$.

emphasize that this substepping is only applied to sedimentation and not the other microphysical process calculations, meaning that hydrometeors can fall multiple vertical levels without undergoing evaporation or other microphysical processes. Since MG1.5 (and MG1) includes an explicit calculation of sedimentation for cloud water and ice only and not precipitation (which is treated diagnostically), there is a limited need for sedimentation substepping because the fall speeds (and hence CFL numbers) of cloud water and ice are small compared to those of rain or snow. Figure 1 also shows the CFL condition for rain sedimentation assuming a $5\,\mathrm{m\,s^{-1}}$ fall speed. Using these lower vertical resolutions we also test sensitivity to the time step and explore time steps up to and slightly beyond the range for CFL stability associated with advection from air motion. Note that the W0 case is a constant condensation rate with no vertical air motion, and hence there is no time step requirement for stability associated with advection from vertical air motion for this case.

The basic cases have fixed droplet and crystal number concentration at 100 and $0.1\,\mathrm{cm^{-3}}$ ($100\,\mathrm{L^{-1}}$) respectively. While the microphysical scheme is built to work with variable number concentrations, for simplicity in an offline framework with no aerosols, we simply fix these values. We perform sensitivity tests of the scheme varying the number concentrations of liquid and ice to explore the sensitivity of the scheme to these parameters, which are prognostic inputs for the GCM version.

We also use these sensitivity tests to explore how the formation of precipitation, in particular the ratio of the accretion and autoconversion process, is sensitive to changes in number concentration and time step. This provides some initial clues about how sensitive the scheme is to changes in drop number, which may be induced by different environments (land, ocean, polluted, pristine).

4. Results

In this section we illustrate the basic results of the new scheme (MG2), and compare it to several other microphysical schemes including MG1.5. We also compare it to the M2005 and T2009 schemes for the different cases. Then we examine the sensitivity of the schemes to time step and vertical resolution.

a. Basic results

Figure 2 shows the cloud (liquid) mass mixing ratio (hereafter "mass" refers to mixing ratio), surface rain rate, rain mass, and rain number for the W1 cloud case from both the MG2 scheme and the M2005 scheme. "Cloud mass" refers to combined liquid and any ice (only present for ice cases below), and liquid and ice to the individual phases. Rain and snow are the falling liquid and ice precipitation species. M2005 is the origin of the MG1 scheme, and with prognostic precipitation for a warm rain case, MG2 should be very similar to M2005. The cloud mass is similar, but MG2 produces significantly more precipitation at the surface than M2005. The difference turns out to be due to the use of a different formula for the saturation vapor pressure between MG2 and M2005. MG2 uses Goff and Gratch (1946) whereas M2005 uses the formulation from Flatau et al. (1992) for computational efficiency. The difference results in approximately a 1% difference in the initial relative humidity, and otherwise the schemes are essentially identical for warm microphysics. While there is sensitivity to small differences in initial relative humidity and hence saturation vapor pressure here, we expect this sensitivity to be reduced for model simulations after a brief initial spinup period.

Figure 3 focuses on the M3 case with an oscillating updraft below an inversion that is colder than 273 K. There is more ice and less liquid in MG2. The precipitation is also significantly higher in MG2 than M2005. This is not surprising since the parameterizations of ice in MG2 and M2005 differ in the treatment of several processes including vapor deposition (Gettelman et al. 2010). However, the patterns and structure are similar.

b. Comparison to other schemes

We now compare MG2 to the MG1.5, M2005, and T2009 schemes, for the cases noted above. We also compare a modified version of the MG2 scheme (MG2-MOD) that uses the saturation vapor pressure calculation from M2005. Figure 4 illustrates the temporally averaged cloud liquid mass, surface rain rate, rain mass, and number for the four different schemes. For this and all subsequent figures, temporal averaging is a simple time average of the entire period. MG2 has similar cloud liquid mass to M2005, slightly larger than T2009, and less than MG1.5. MG2-MOD (red) has nearly identical results as M2005 (green), demonstrating that the differences between M2005 and MG2 for warm microphysics are because of differences in saturation vapor pressure. Nonetheless, MG2 and M2005 have similar precipitation mass and rain number for this case, while T2009 has lower averaged rain mass and number. MG1.5 looks different in character to all the other schemes. The surface precipitation is consistent with the process rates. In particular, MG2 has a high accretion rate compared to MG1.5 (Fig. 4f), and the larger precipitation rate is consistent with this.

MG1.5 cloud liquid mass is large (Fig. 4a), it produces precipitation early (Fig. 4b), and the accretion rate is relatively small and peaked near cloud base (Fig. 4e),

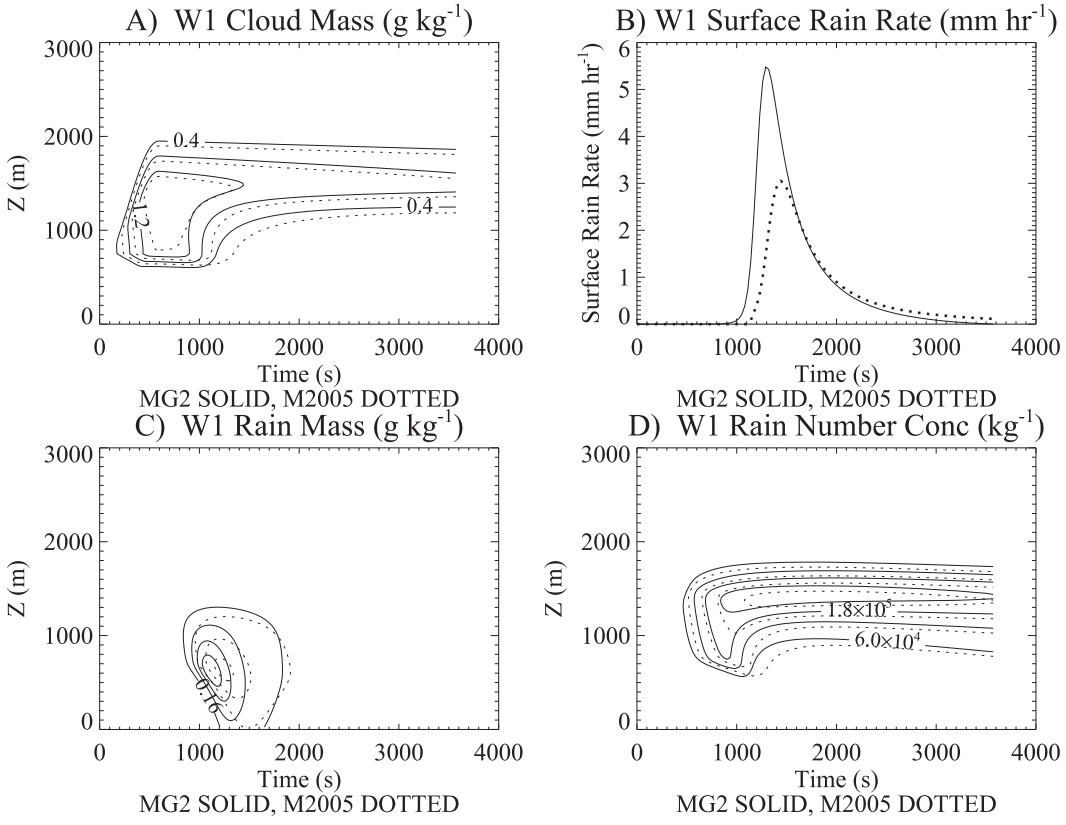

FIG. 2. Warm 1 (W1) case results for (a) cloud liquid mass (contour interval 0.4 g kg^{-1}), (b) surface precipitation rate, (c) warm rain mass (contour interval 0.16 g kg^{-1}), and (d) rain number (contour interval 6×10^4 kg^{-1}) from MG2 (solid) and M2005 (dashed).

compared with the other schemes. MG1.5 has a more significant contribution from autoconversion than MG2 or M2005. It is not as peaked at cloud top, and larger at cloud base than any other scheme examined. MG1.5 is the only scheme examined with diagnostic precipitation.

Another difference between MG2 and MG1.5 is that we have included the evaporation of rain number in MG2 as in M2005. We have investigated the impact of this change, and in the W1 case it produces answers very similar to the MG2 case in Fig. 4, with the only difference being a few percent less rain mass and number, and about 10% more integrated rain (slightly higher precipitation efficiency) since reduction of rain number with evaporation below cloud means larger size drops and faster fall speeds. Peak rain production is similar; the effect is most apparent when the cloud is dissipating.

Figure 5 shows similar plots for the mixed phase M3 case, which also includes ice mass. Cloud mass has been segmented into liquid and ice. MG2 and MG1.5 have less liquid than T2009 or M2005. The structure of the clouds is similar between the schemes, but MG2 and MG1.5 have very similar liquid mass (Fig. 5a) while the M2005 and T2009 schemes have larger liquid mass. The MG2-MOD scheme has a larger liquid mass and is closer to M2005. MG2 and MG1.5 have significantly more ice (mass mixing ratio) than M2005. This may be due to the saturation vapor pressure difference between the MG schemes and M2005 discussed above. MG2-MOD and T2009 have very little ice mass in these cases. Total precipitation (Fig. 5c) is also higher in MG2 and MG1.5. This surface precipitation includes the ice phase precipitation (snow), so the higher ice mass appears to be important in the resulting precipitation.

A "pure" ice case was also performed (Ice 1, Fig. 6) to explore how the schemes would work at temperatures where only ice is present. An updraft similar to the W1 case is placed in a domain up to 12 km with a humid layer from 6 to 10 km (Fig. 6a). The temperature at the base of the cloud is 215 K, so no liquid is present. The schemes behave differently, with large differences in ice mass (Fig. 6b) and precipitation. The differences between MG1.5 (dark blue) and MG2 (red) are mainly due to a different setting of the ice autoconversion parameter (DCS). In these experiments with MG1.5 DCS = 250 μm, while in

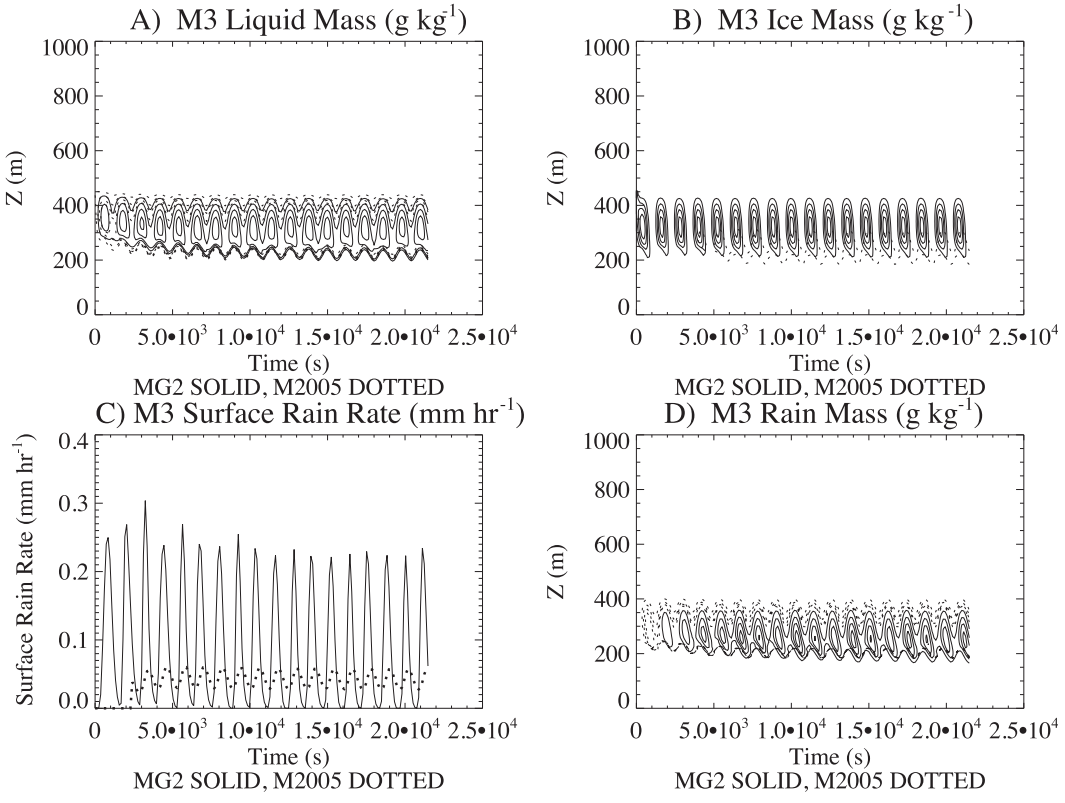

FIG. 3. Mixed 3 (M3) case results for (a) cloud liquid mass (contour interval 0.4 g kg^{-1}), (b) cloud ice mass (contour interval 0.016 g kg^{-1}), (c) surface precipitation, and (d) rain mass (contour interval 1.2×10^{-4} g kg^{-1}) from MG2 (solid) and M2005 (dashed).

MG2 DCS = 90 μm to reduce ice cloud mass for radiative energy balance in global simulations. A simulation using MG2 with DCS = 250 μm (black in Fig. 6) has nearly the same relative humidity (Fig. 6a) and identical ice mass (Fig. 6b: the black and blue dotted lines overlap) as MG1.5. There are significant differences for the precipitation mass, but in all schemes it sublimates before hitting the ground. All schemes form a cloud in a similar layer, but have very different precipitation properties.

c. *Time step sensitivity*

Next we explore the sensitivity of the MG2 scheme to time step. For these tests, the number of vertical levels is reduced to 6 (500 m per level). We use the same initial profile as the W1 case, but we set zero vertical air velocity and instead apply a fixed condensation rate of 5×10^{-7} kg kg^{-1} s^{-1}. All four hydrometeors (liquid, ice, rain, and snow) sediment in the microphysics. They are advected by grid scale vertical air motion in the dynamical core (not in the microphysics). Since the thermodynamic and dynamic fields resolved by GCMs vary slowly compared to those in high-resolution models, this setup is more applicable to GCMs. GCMs apply a constant condensation rate over long (10–30 min) time steps like this steady forcing case. Figure 7a indicates that the MG2 parameterization is relatively insensitive to time step out to 120 s for cloud liquid mass. Here the control case has different time steps: DT = 1 s. Differences are also clear in rain mass (Fig. 7c). The varying solution with time step seems to occur because of sedimentation. Numerical stability is assured by substepping, but for a 5 m s^{-1} fall speed, rain can fall through a 500-m grid box in 100 s (Fig. 1) and hence can fall several levels without undergoing evaporation or other microphysical processes, since only sedimentation is substepped and not the rest of the microphysical calculations. Thus, we would expect solutions may be different beyond a 100-s time step, especially for rain mass (Fig. 7c) and rain number (Fig. 7d). Different rain mass then affects cloud water through accretion (Fig. 7f), which subsequently alters autoconversion (Fig. 7e) and accretion rates. Precipitation rate (Fig. 7b) approaches the same value regardless of time step, as it is a function of the condensation rate. The oscillations that appear in the first period (up to 2×10^4 s) are a consequence of different

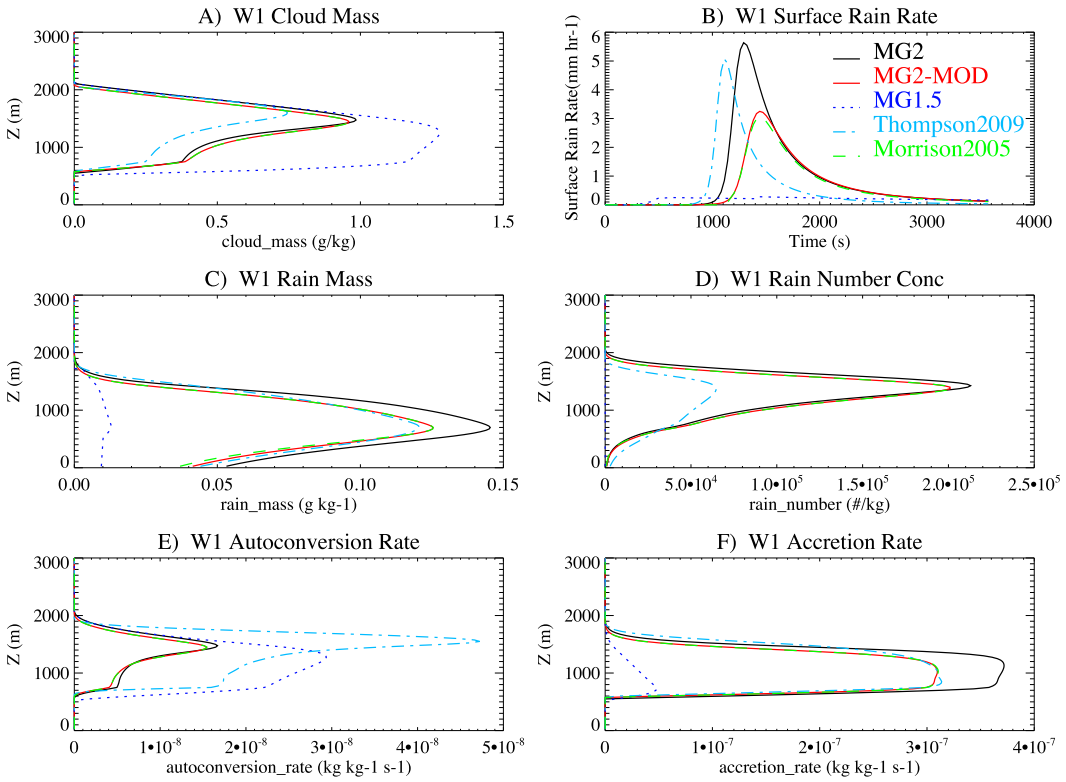

FIG. 4. Warm 1 (W1) case comparisons of temporally averaged (a) cloud liquid mass, (b) surface precipitation rate (not temporally averaged), (c) rain mass, (d) rain number, (e) autoconversion rate, and (f) accretion rate from MG2 (solid black), MG2-MOD (solid red), T2009 (dotted–dashed cyan), M2005 (dashed green), and MG1.5 (dotted dark blue).

numbers of vertical levels (NZ); the NZ = 6 setup, and are not seen for NZ = 15 and higher vertical resolutions (see below).

Perhaps more relevant for application of the scheme in a GCM is to look at the sensitivity of the final liquid water path (LWP) and precipitation rate over the last 2 h for the steady forcing case (W0). LWP does not include rainwater. Figure 8b indicates that the precipitation rate in MG2 is insensitive to time step, varying by at most 10% and generally only a few percent. This is expected since we use a constant condensation rate. However, LWP (Fig. 8a) seems to increase with time step in all schemes. Note that the precipitation rate in MG1.5 (the only scheme with diagnostic precipitation) increases more (40%), with a compensation from a smaller increase in LWP. Thus MG1.5 precipitation seems more sensitive to time step, again, likely due to the different processes acting on falling precipitation in the diagnostic versus prognostic treatment. The LWP increase in all schemes is likely driven by the formulation of the KiD test forced by constant condensation: the longer the time step, the more condensation occurs in each step. This means that, given a condensation rate, the microphysics generates the same precipitation rate regardless of time step, but the total condensation in each step is larger (as is the total precipitation), resulting in a higher LWP and reduced precipitation efficiency. For the steady forcing case, in equilibrium the surface precipitation rate must equal the vertically integrated applied condensation rate. Integrating the condensation rate over the 3000-m vertical domain yields about 4.2 mm h^{-1}, similar to the precipitation rate in Fig. 8b. The role of time stepping in the coupling between bulk condensation (treated outside of the microphysics code) and microphysics is explored further in Part II.

The other schemes perform similarly across time steps. This is expected because the rain rate has to balance the net condensation rate (which is about 4.2 mm h^{-1}) in equilibrium. Note, however, that true equilibrium cannot be achieved in these simulations because there is no cooling applied to balance the net latent heating associated with surface precipitation. Nonetheless, the point is not to test schemes under exact equilibrium but rather to test them under slowly varying thermodynamic conditions (steady forcing). The final precipitation rate is different for MG1.5, especially for

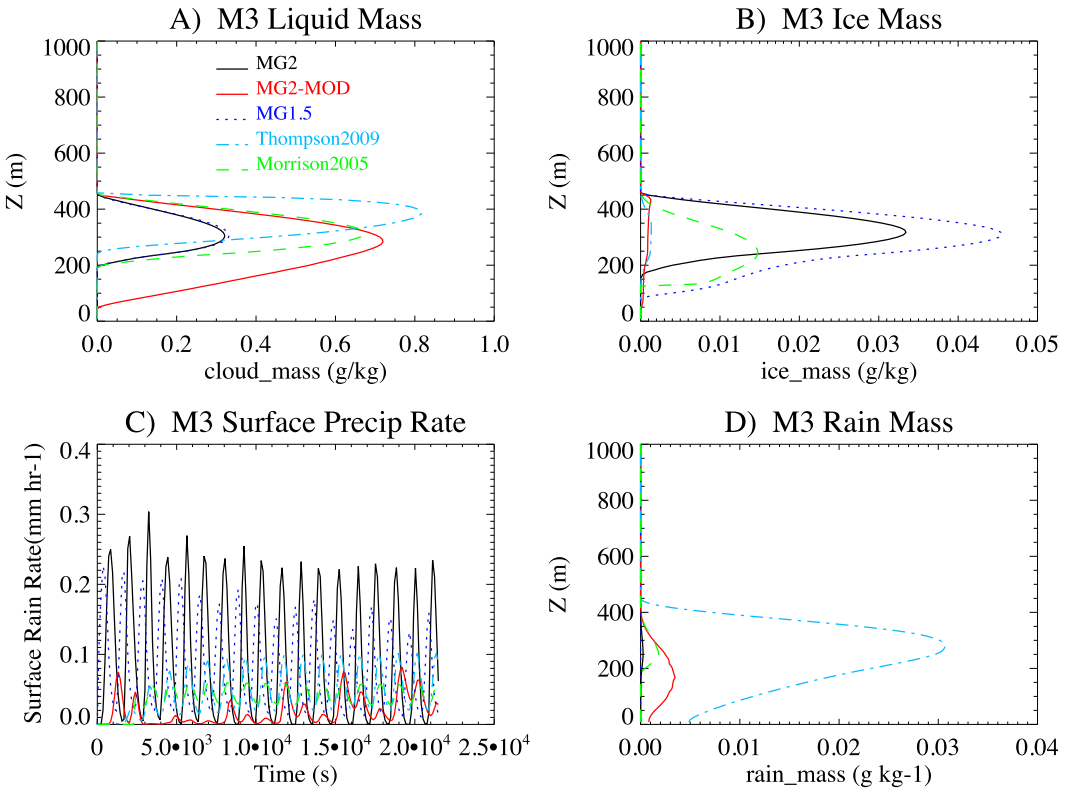

FIG. 5. Mixed 3 (M3) case comparisons of temporally averaged (a) cloud liquid mass, (b) cloud ice mass, (c) surface precipitation (not temporally averaged), and (d) rain mass from MG2 (solid black), MG2-MOD (solid red), T2009 (dotted–dashed cyan), M2005 (dashed green), and MG1.5 (dotted dark blue).

shorter time steps, indicating a more significant departure from equilibrium for this scheme. The treatment of substepping with prognostic precipitation in MG2 (for CFL in sedimentation) will lead to differences compared to diagnostic precipitation in MG1.5 (which has a different treatment of sedimentation and is not substepped in this way). Thus, we do not expect the prognostic and diagnostic schemes to converge. MG2 has a reduced sensitivity compared to MG1.5 for the precipitation rate in Fig. 8.

d. Vertical resolution sensitivity

Another aspect of sensitivity is with respect to vertical resolution. Figure 9 shows sensitivity of the results for cloud liquid mass to changes in vertical resolution for the Warm 1 case and the MG2 scheme with a 1-s time step. The NZ = 120 case is the same as the MG2 case in Fig. 4. Results are very similar for this case from 120 to 30 levels, while the 15- and 6-level cases (200- and 500-m vertical grid spacings) are different. These cases have a difficult time resolving the peak in cloud mass in the W1 case (Fig. 9a). This translates through the other microphysical quantities: the cases from 120 to 30 levels are very similar while the lower-resolution cases are different. It is likely that the differences are due to the coarse vertical averaging of the initial temperature and humidity profile for this case (which features a humid layer from 600- to 2000-m altitude). For the six-level (500-m resolution) case, the vertical features are not sufficiently resolved, so the results are different.

Table 2 illustrates the average LWP and total precipitation, as well as the precipitation efficiency (PE) estimated from the total saturation adjustment such that $\mathrm{PE} = \overline{R}/\overline{Q_{\mathrm{sat}}}$, where $\overline{R}$ is the time integrated rain rate and $\overline{Q_{\mathrm{sat}}}$ is the time and vertically integrated net condensation rate. The results indicate a sensitivity of LWP to vertical resolution, with higher LWP at higher vertical resolution. The total integrated precipitation varies by 20%–30%, but not monotonically. PE is fairly constant at all vertical resolutions. Except for the NZ = 15 (200 m) case, the precipitation efficiency is within 10%. Vertical resolution sensitivity of PE is higher in MG1.5; it varies between 0.16 and 0.04 and is also not monotonic.

Sensitivity to vertical resolution is also examined for the steady forcing (W0) case (Fig. 10). Here DT = 1 s for all cases, so the NZ = 6 case corresponds to the DT = 1 case in Fig. 7. The final rain rate is sensitive to vertical resolution (Fig. 10b) for NZ = 15 or 6 (200 or 500 m), but

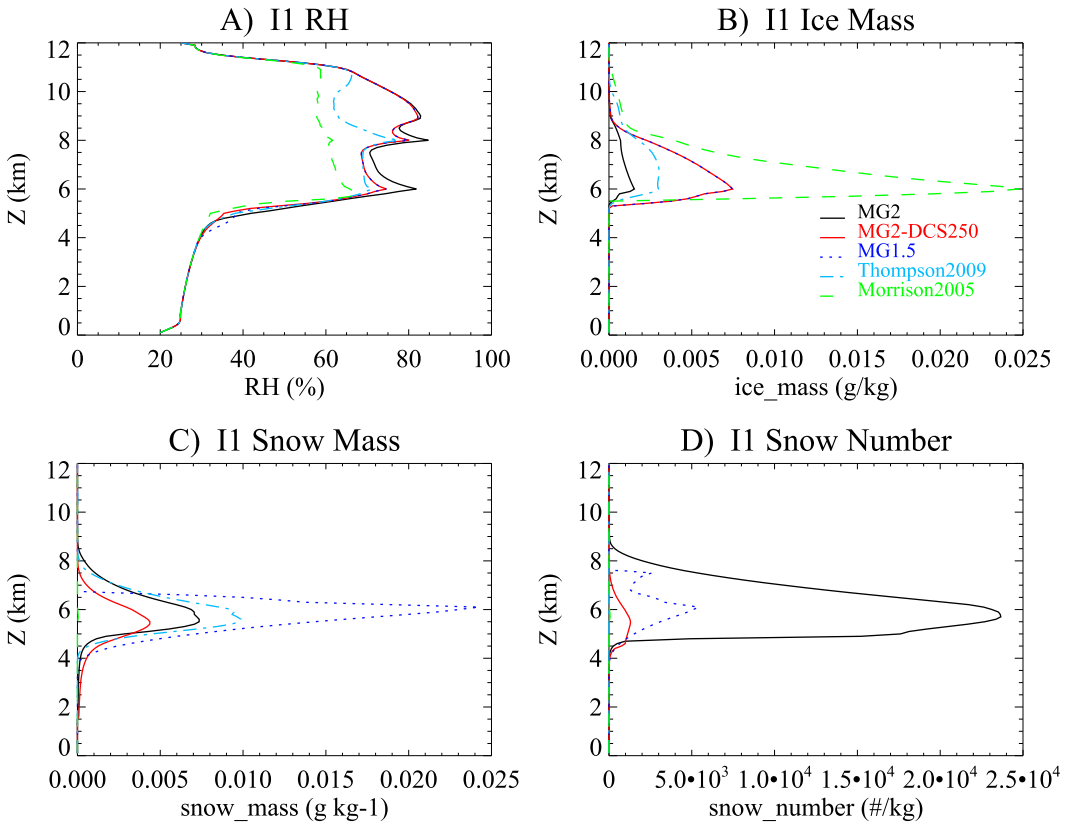

FIG. 6. Ice 1 (I1) cirrus case comparisons of temporally averaged (a) relative humidity, (b) cloud ice mass, (c) snow mass, and (d) snow number from MG2 (solid black), MG2 with DCS = 250 μm (solid red), T2009 (dotted–dashed cyan), M2005 (dashed green), and MG1.5 (dotted dark blue).

fairly insensitive for NZ = 30 to 120 (100 to 25 m). However, the cloud liquid mass changes significantly (Fig. 10a), mostly due to not resolving the thin cloud layer at the top of the simulation induced by the balance of condensation and autoconversion and accretion. The rain mass (Fig. 10c) is fairly constant with resolution except at the top and bottom level, and depends mostly on accretion (Fig. 10f), which is an order of magnitude higher than autoconversion (Fig. 10e). Rain number (Fig. 10d) is strongly dependent on autoconversion.

The vertical sensitivity of the final ("near-equilibrium") LWP and rain rate for all of the different microphysics schemes is illustrated in Fig. 11. MG2 and M2005 have nearly identical performance across vertical spacings from 25 to 500 m (from NZ = 120 to 6). There are decreases in LWP with decreasing vertical resolution (increased spacing) for all the schemes, less so in T2009 but more so in MG1.5 (Fig. 11a) at small spacings (<200 m), and increases in LWP with larger spacings. The final rain rate is also sensitive to resolution (Fig. 11b) in almost exactly the same way in MG2, M2005, and T2009 (the three schemes with prognostic precipitation). These differences map into the differences in cloud liquid mass seen in Fig. 10. Departure from true steady-state conditions, as noted above, is reflected by some differences in the final surface precipitation rate. Moreover, the constant condensation rate (specified in $\mathrm{kg\,kg^{-1}\,s^{-1}}$) is applied at different levels as the vertical resolution is modified, leading to small differences in the vertical integral of condensation rate by ~2%.

On the whole, the new scheme has limited sensitivity across nearly a range of magnitude in vertical resolution up to GCM resolution in the lower atmosphere, and across two orders of magnitude in time step at least to 900 s, as long as basic numerical stability criteria are satisfied.

5. Sensitivity and process rates

We now explore the sensitivity of the scheme to perturbations in cloud droplet and crystal number concentrations and analyze the process rates for warm rain formation. As noted by Gettelman et al. (2013), the relationship between the autoconversion of drops to

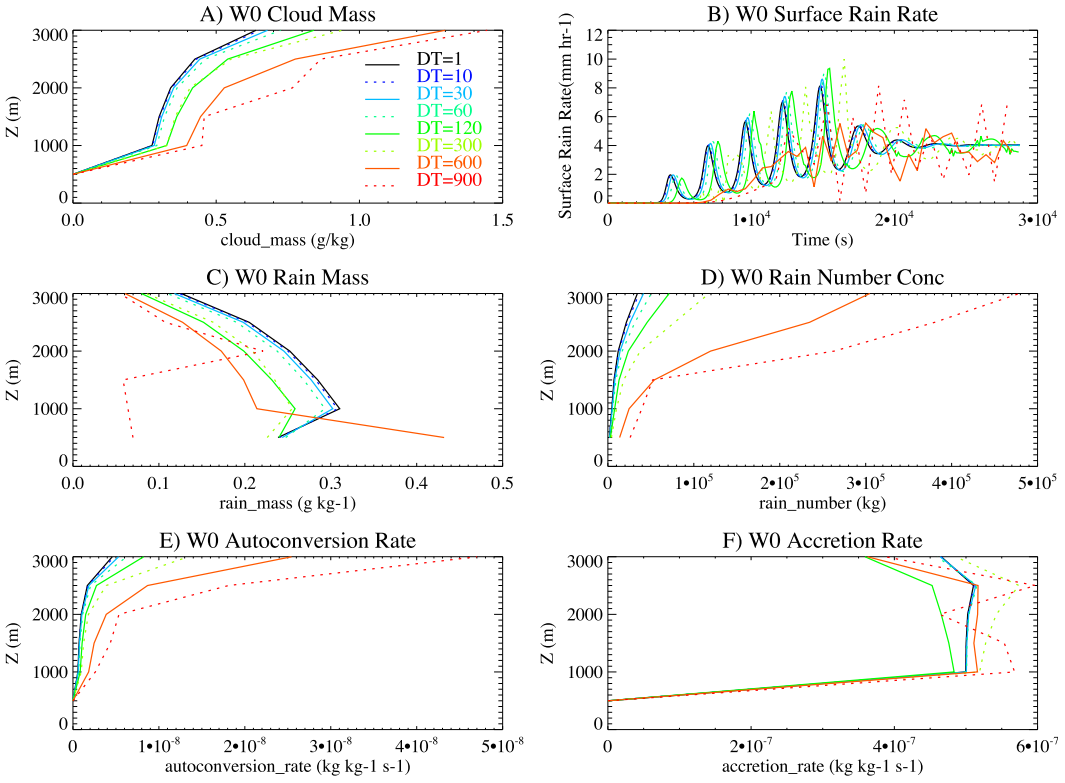

FIG. 7. MG2 fixed condensation rate (W0) case comparisons of temporally averaged (a) cloud liquid mass, (b) surface rain rate (not temporally averaged), (c) rain mass, (d) rain number, (e) autoconversion rate, and (f) accretion rate from different time steps with NZ = 6 (DZ = 500 m). Lines indicate different time steps (DT) from 1 to 900 s as noted in the legend.

precipitation and accretion of drops by precipitation in MG1.5 indicates higher relative and absolute rates of autoconversion. The parameterization of Khairoutdinov and Kogan (2000) assumes autoconversion is inversely related to droplet number ($N_c^{-1.79}$), but increases with cloud mass ($q_c^{2.47}$), while accretion is a function of cloud and rain mass [$(q_c q_r)^{1.15}$]. If N_c is constant, unless q_r is large, then autoconversion will remain important even at large LWP. This is seen in the simulations by Gettelman et al. (2013) in CAM5, and may result from the diagnostic treatment of precipitation in MG1.5 (small q_r seen by the microphysics; e.g., Fig. 4c). This

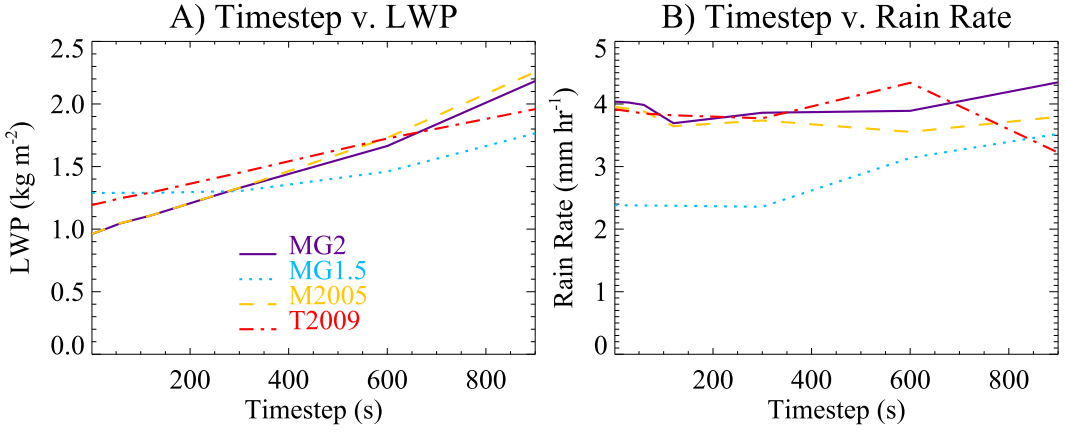

FIG. 8. Steady-state (W0) case (a) LWP and (b) rain rate vs time step for MG2 (solid purple), MG1.5 (dotted cyan), M2005 (dashed yellow-orange), and T2009 (dotted–dashed red).

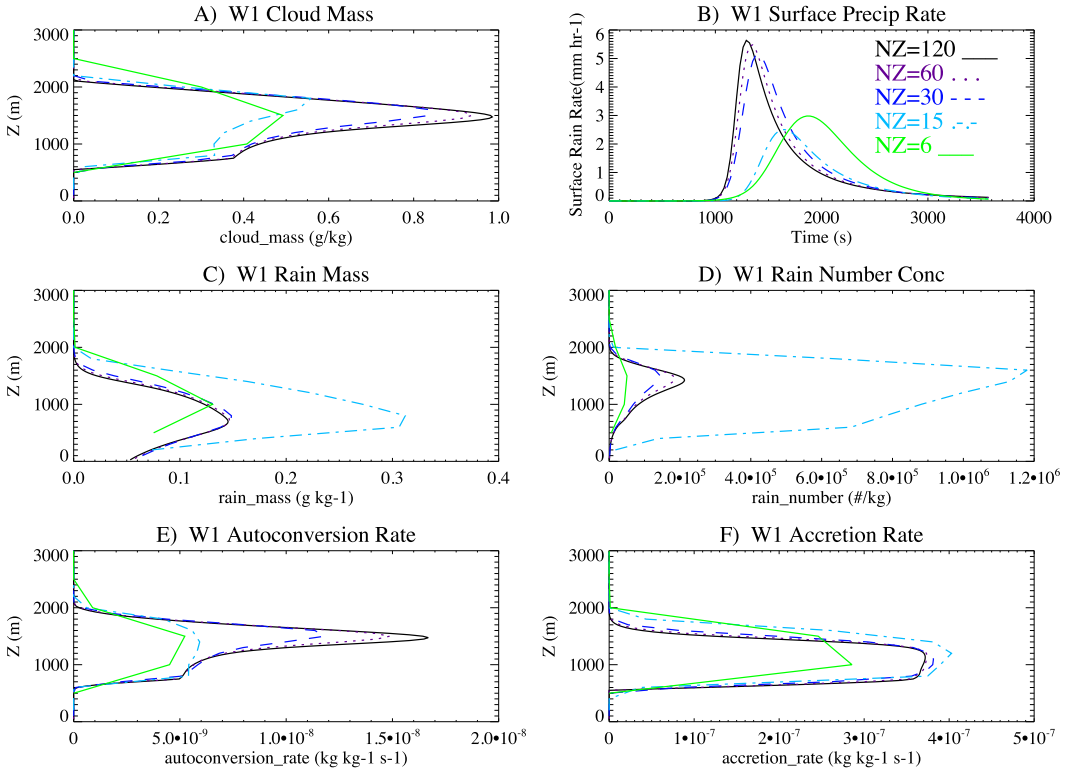

FIG. 9. MG2 W1 case comparisons of temporally averaged (a) cloud liquid mass, (b) surface rain rate (not temporally averaged), (c) rain mass, (d) rain number, (e) autoconversion rate, and (f) accretion rate with different numbers of vertical levels (NZ): NZ = 120 (solid black), NZ = 60 (dotted purple), NZ = 30 (dashed dark blue), NZ = 15 (dotted–dashed light blue), and NZ = 6 (solid green). All have DT = 1 s.

may also affect the sensitivity of the scheme (precipitation and total water path response) to perturbations of drop number. We examine this in more detail below. Note that we are focusing in this work on just MG2 (and differences from MG1.5). A more complete analysis of process rates and sensitivity to droplet number in M2005 and T2009, as well as other schemes, has recently been provided by Hill et al. (2014, manuscript submitted to *J. Adv. Model. Earth Syst.*).

a. Effect of cloud droplet and crystal number

First we examine the effects of changing drop and crystal number concentrations in the simulations. These are specified in the microphysics used in the KiD model, as a proxy for aerosols. High drop numbers are associated with high aerosol loading yielding large numbers of cloud condensation nuclei (CCN) and ice nuclei (IN). The process rates in the microphysical parameterization are dependent on both cloud mass and drop number. Autoconversion of cloud to rain drops is assumed to be an inverse function of number (Khairoutdinov and Kogan 2000), so increasing drop number should reduce precipitation and increase cloud liquid mass, all else being equal. This is clearly illustrated in Fig. 12 for the W1 case with MG2. Drop number concentration is varied from 10 to 2000 cm^{-3}. The $N_c = 100\,cm^{-2}$ case is the same as the control MG2 case in Fig. 4 and the NZ = 120 and DT = 1 for the W1

TABLE 2. Vertical resolution sensitivity: MG2 Warm 1 case, DT = 1 s. Values are temporal averages for LWP, and integrated total for precipitation.

Vertical spacing (m)	No. of levels	LWP ($kg\,m^{-2}$)	Total precipitation ($kg\,m^{-2}$)	Precipitation efficiency
25	120	0.84	0.87	0.33
50	60	0.82	0.88	0.33
100	30	0.78	0.90	0.36
200	15	0.61	0.65	0.26
500	6	0.62	0.76	0.36

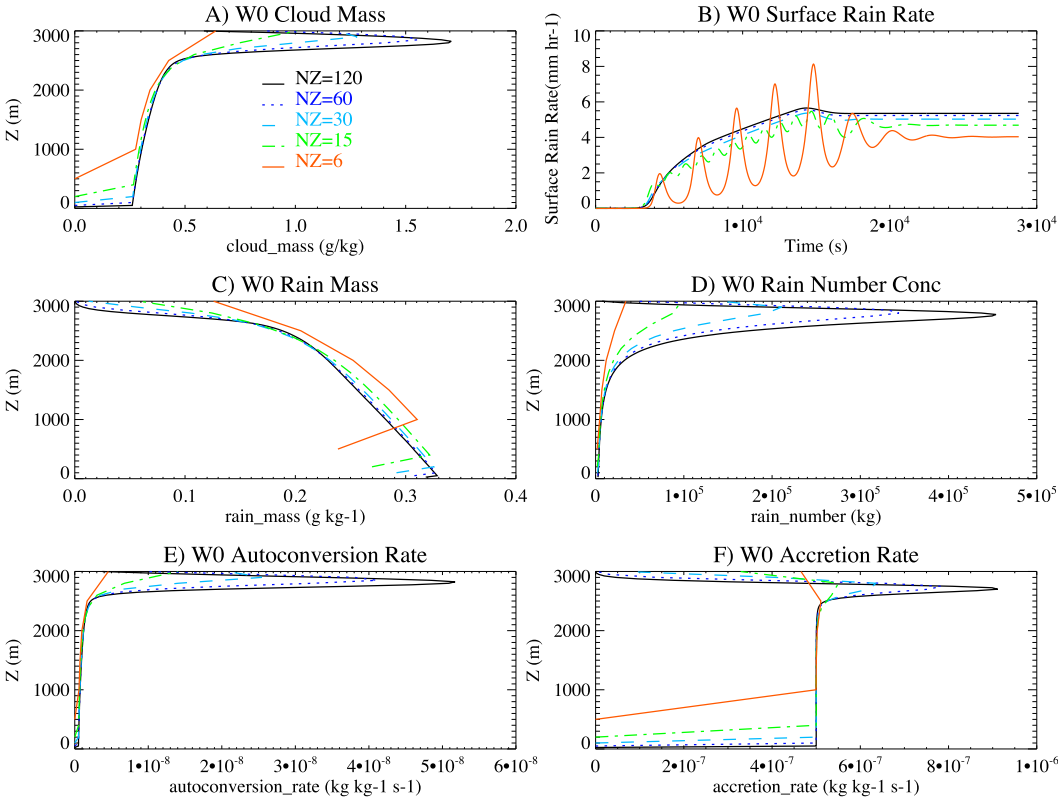

FIG. 10. MG2 constant condensation (W0) case comparisons of temporally averaged (a) cloud liquid mass, (b) surface rain rate (not temporally averaged), (c) rain mass, (d) rain number, (e) autoconversion rate, and (f) accretion rate from different time steps with NZ = 120 (solid black), NZ = 60 (dotted dark blue), NZ = 30 (dashed cyan), NZ = 15 (dotted–dashed green), and NZ = 6 (solid orange). DT = 1 s for all.

MG2 case in Fig. 9. As drop number increases, cloud mass (Fig. 12a) increases, while surface precipitation (Fig. 12b) decreases. Precipitation mass (Fig. 12c) and number (Fig. 12d) also decrease, as do autoconversion (Fig. 12e) and accretion (Fig. 12f).

The effect of altering ice crystal number concentration (N_i) in MG2 is illustrated in Fig. 13 for the M3 case with constant $N_c = 100\,\mathrm{cm}^{-2}$. Increasing ice number increases ice mass (Fig. 13b). However, it has a larger absolute effect on liquid cloud mass (Fig. 13a): increasing

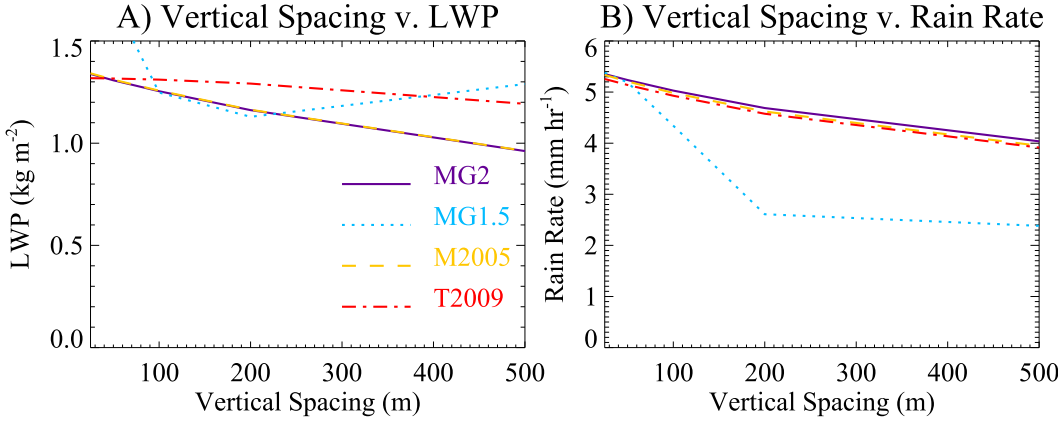

FIG. 11. Steady-state case (a) LWP and (b) rain rate vs vertical resolution for MG2 (solid purple), MG1.5 (dotted cyan), M2005 (dashed yellow-orange), and T2009 (dotted–dashed red).

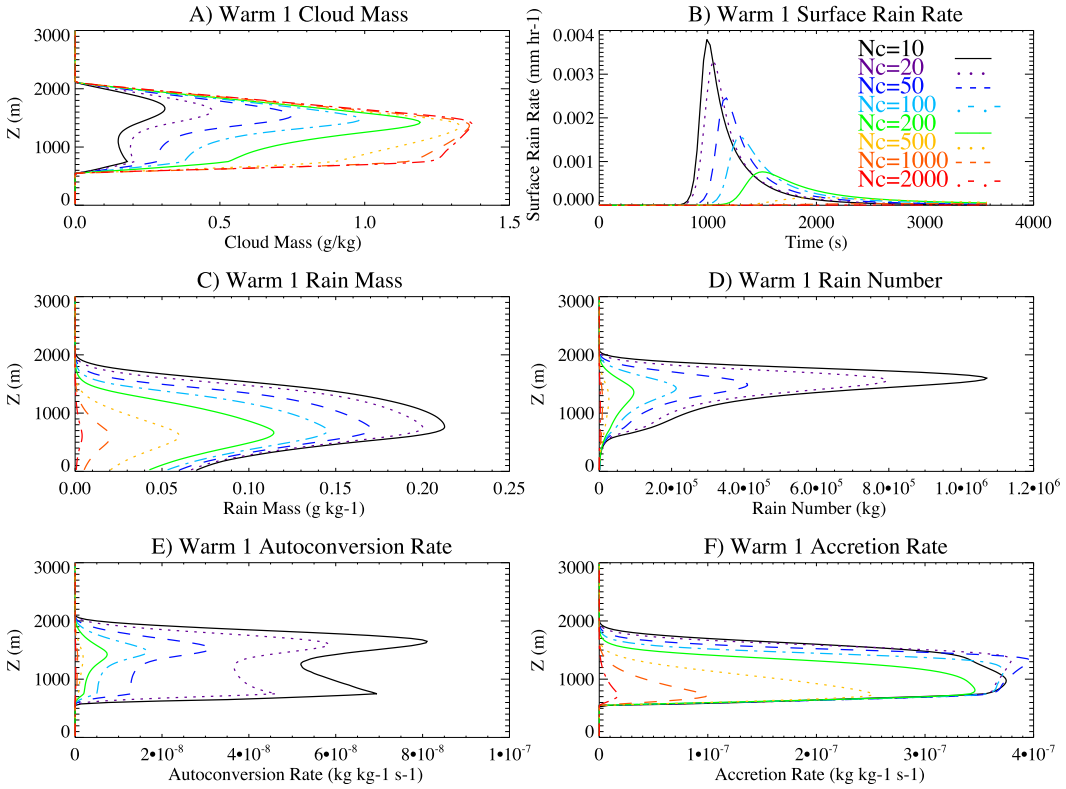

FIG. 12. Warm 1 (W1) case comparisons with MG2 of temporally averaged (a) cloud liquid mass, (b) surface rain rate (not temporally averaged), (c) rain mass, (d) rain number, (e) autoconversion rate, and (f) accretion rate with different number concentrations (colored lines) from 10 to 2000 cm^{-3}.

ice mass and ice number decreases liquid cloud mass substantially. Precipitation at the surface (Fig. 13c) and suspended rain mass (Fig. 13d) also decrease with increasing ice number, likely because of the reduced cloud liquid mass.

Note how a small absolute change in ice mass ($0.03\,g\,kg^{-1}$) results in larger absolute ($0.20\,g\,kg^{-1}$) changes in liquid mass. In the microphysics, higher ice number and mass means a more active vapor deposition process (larger tendency) and this reduces the remaining liquid via the Wegener–Bergeron–Findeisen mechanism. Ice falls out rapidly as it grows and depletes vapor and liquid rapidly. The relative change in ice and liquid mass is about the same.

Precipitation efficiency (PE) is another metric of the balance of microphysical process rates. PE is defined as the integrated surface precipitation rate divided by the time integrated total condensation rate in Figs. 14a and 14d. We also plot the mean liquid water path (Figs. 14b,e) not including rain and the total time integrated surface precipitation (Figs. 14c,f). Note that integrated total condensation rate and integrated precipitation at the surface are different (by the evaporation). Quantities are plotted from MG1.5 and MG2 as a function of drop number concentration in Fig. 14. Each point represents one fixed drop number concentration run (simulations in Fig. 12).

As expected in this kinematically constrained case, precipitation efficiency decreases with increasing number concentration (Fig. 14a). This also occurs with MG1.5 (Fig. 14d). Some of the cases are different. For the W1 case, the PE decrease with LWP (dPE/dLWP) is smaller with MG2 than MG1.5, while the other cases (W2 and W3) are about the same, although MG2 has more nonzero PE (owing to higher precipitation rates) up to higher number concentrations in these cases. Stated another way, PE tends to be higher for a given LWP in MG2 than MG1.5.

Notably, the mean LWP increases at a more gradual rate with number concentration in MG2 from MG1.5 (Figs. 14b,e). The increase can also be seen in Fig. 12, which uses the same simulations. At lower number concentrations ($<100\,cm^{-3}$), MG2 appears to have lower LWP sensitivity to drop number. This is also true of total surface precipitation (Figs. 14c,f). Total precipitation falls with increasing number concentration in MG2 and MG1.5. Case W1 has higher precipitation for larger LWP in MG2, while cases W2 and W3 are similar between MG1 and MG2.

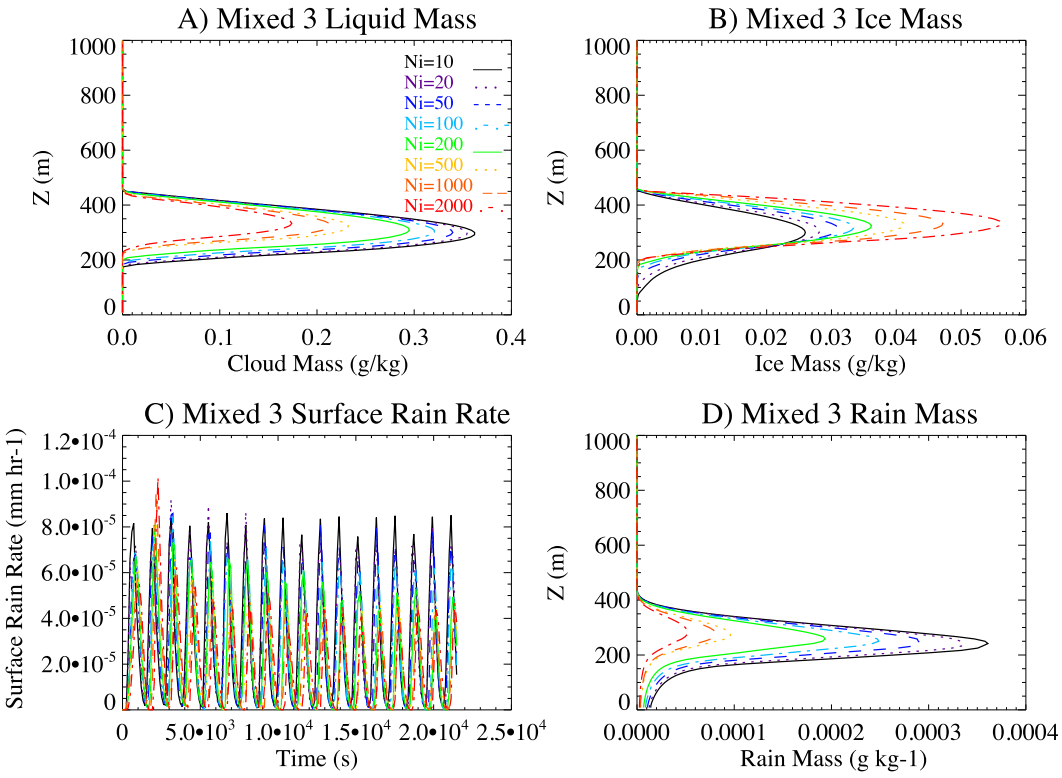

FIG. 13. Mixed 3 case comparisons with MG2 of temporally averaged (a) cloud liquid mass, (b) cloud ice mass, (c) surface rain rate (not temporally averaged), and (d) rain mass with different number concentrations for ice crystals (colored lines) from 10 to 2000 L^{-1}. Fixed drop number of $N_c = 100\,cm^{-2}$.

We have also examined PE, LWP, and total precipitation in M2005 and T2009 as a function of changing droplet number concentration. Results look qualitatively and quantitatively similar to MG2, with PE highest for low number concentrations at about 0.6, 0.2, and 0.1 for cases W1, W2, and W3 respectively. Mean water path (LWP) also increases at a steady rate in M2005 and T2009, and total precipitation declines with number concentration to near zero precipitation at $1000\,cm^{-3}$.

b. *Process rates*

Finally, we examine the detailed process rates governing precipitation formation in MG2. The fundamental task of the microphysical parameterization is to speciate and partition cloud condensate, and to calculate the precipitation processes. Precipitation is a sink for cloud condensate. Focusing on the warm rain process, the collision and coalescence of cloud droplets to form embryo rain drops is parameterized by the autoconversion of cloud to rain. The accretion process represents the collection of cloud droplets by existing rain drops. Gettelman et al. (2013) show how the GCM version of the MG1.5 microphysics seems to have significantly more autoconversion at a given liquid water path than calculations from observed drop size distributions.

This is illustrated for the warm rain cases (W1–W3) in Fig. 15. The accretion and autoconversion rates are vertically averaged, and the ratio is averaged across the entire cloud layer for each case, and compared to the average liquid water path (without rain). The different fixed number concentration simulations have a diversity of LWP (Fig. 12a). In MG2 (Fig. 15a), accretion dominates over autoconversion, but not for MG1.5 (Fig. 15b). In general, the ratio of accretion to autoconversion is much higher in MG2 than MG1.5 (Fig. 15) because the accretion rate is a function of the cloud liquid mass and rain mass, while the autoconversion rate is a function of the cloud liquid mass and number (Khairoutdinov and Kogan 2000). So with prognostic rain, accretion is increased substantially relative to autoconversion in MG2 (Fig. 15). M2005 (Fig. 15c) is very similar to MG2. For the W1 case, T2009 (Fig. 15d) is also similar to MG2 and M2005. For the W2 and W3 cases, accretion increases even more rapidly with LWP. A similar result can be obtained by varying the updraft speed to get different liquid water paths rather than the number concentration.

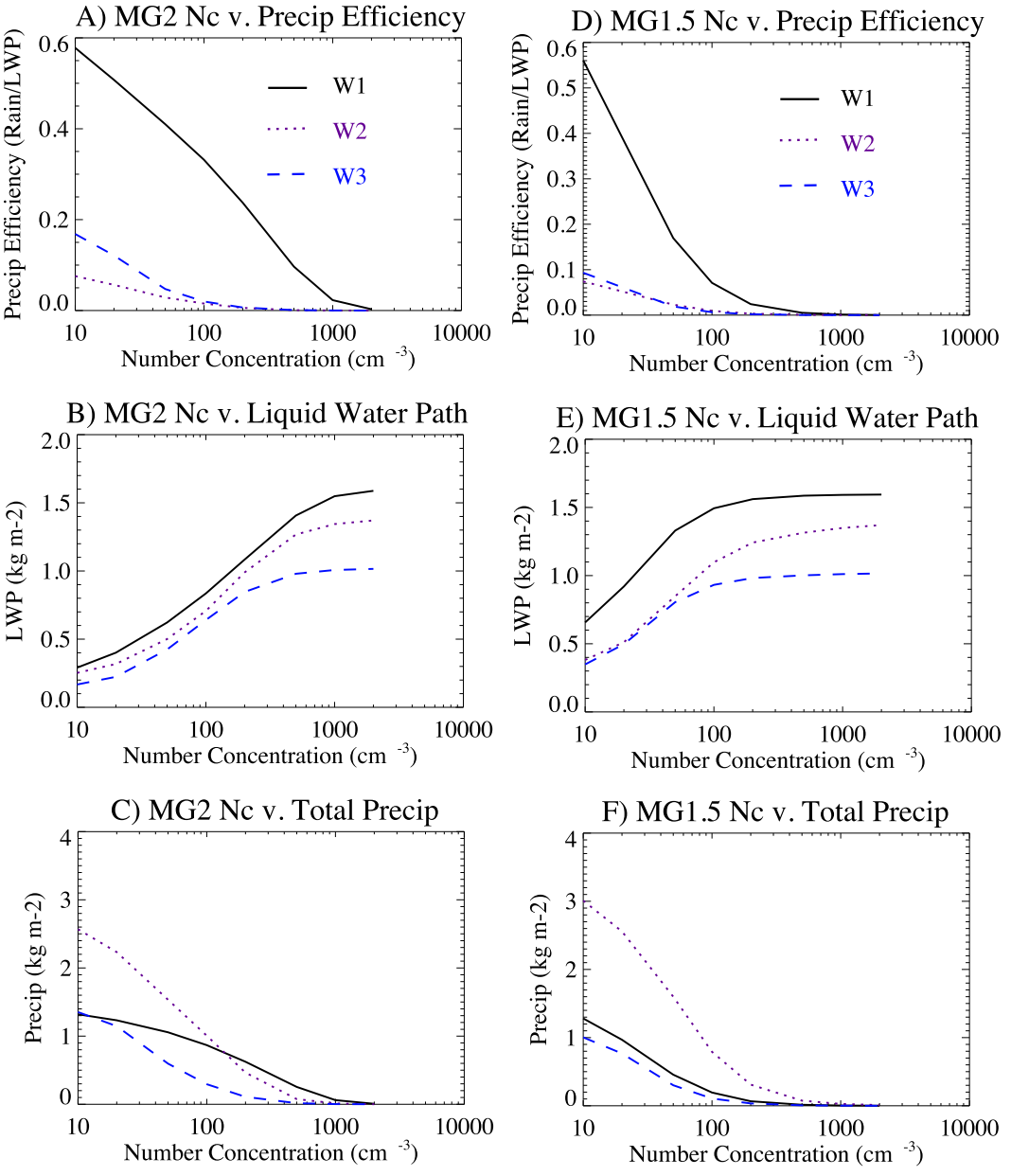

FIG. 14. Warm 1 (W1: black solid), Warm 2 (W2: purple dotted), and Warm 3 (W3: blue dashed) case comparisons of drop number sensitivity of (a),(d) precipitation efficiency, (b),(e) liquid water path (not including rain), and (c),(f) integrated total precipitation, using (left) MG2 and (right) using MG1.5.

6. Summary and conclusions

We have added prognostic precipitation to the existing microphysical scheme of MG2008 for use in global climate models. The scheme has been tested in an offline driver and compared to the original version with diagnostic precipitation (MG1.5) as well as two other schemes developed for cloud and mesoscale models (M2005 and T2009). The scheme is similar to M2005, and with appropriate constraints can recover nearly identical solutions for warm rain cases to M2005. Because the evaporation of rain number and the sedimentation and substepping of processes is not the same between MG1.5 and MG2, we do not expect them to converge even at longer time steps.

We have tested sensitivity to time step and vertical resolution. The time step sensitivity is bound up with interactions between the condensation and microphysics. When forced with a steady condensation rate, MG2 produces limited sensitivity of surface precipitation for

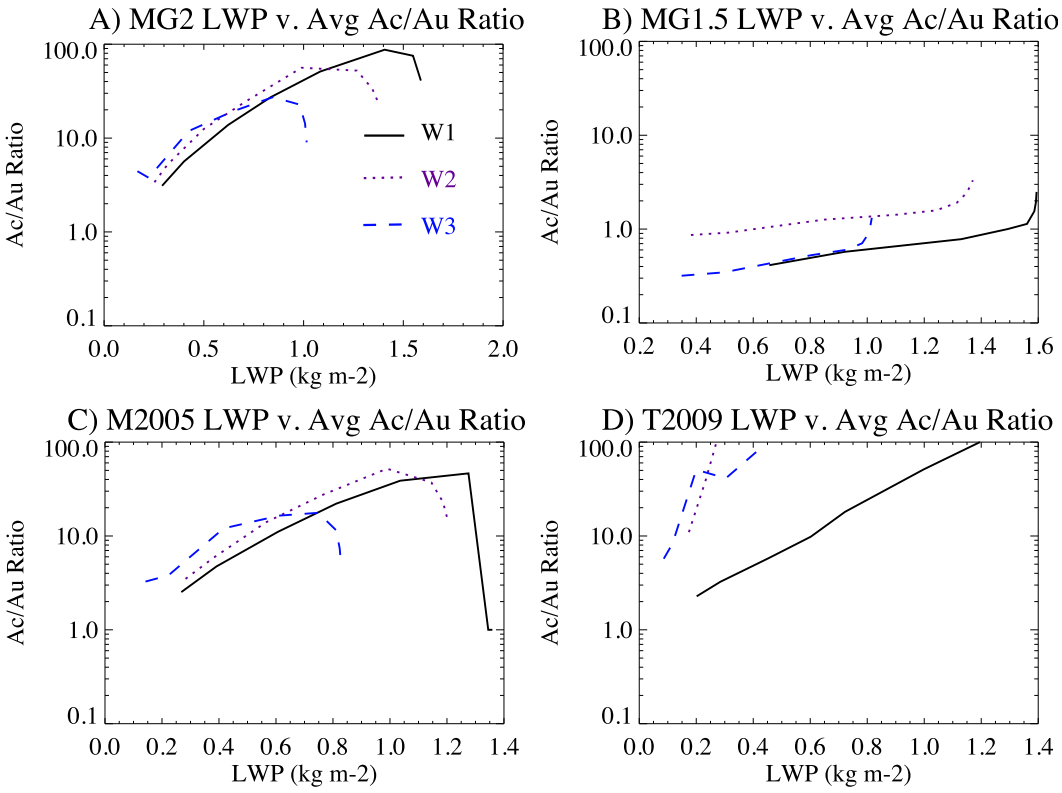

FIG. 15. Warm 1 (W1: black solid), Warm 2 (W2: purple dotted), and Warm 3 (W3: blue dashed) case comparisons of mean LWP vs Ac/Au ratio using simulations with different N_c to provide variance in LWP for (a) MG1.5, (b) MG2, (c) M2005, and (d) T2009.

time steps from 1 to 900 s, approaching the time steps used in a GCM (which has similar steady condensation rates over a time step). In addition, all the different schemes with prognostic precipitation in this case produce nearly the same final (quasi-equilibrium) precipitation rate for time steps of 300 s or less. Note that these simulations were not in exact equilibrium, especially for MG1.5, which explains differences in the final precipitation rate. MG1.5 exhibits more sensitivity of surface precipitation rate to time steps longer than 300 s than the other schemes with prognostic precipitation. MG1.5 has a smaller precipitation rate for time steps below 300 s. LWP, however, increases monotonically with time step in all of the schemes (except for MG1.5 at time steps shorter than 300 s).

Sensitivity to vertical resolution is low between 25 and 100 m with prognostic precipitation (all schemes except MG1.5). At 200- and 500-m vertical grid spacing, results vary. This is partially due to differing representations of the initial thermodynamic profiles at lower resolution. It is not clear that there is a problem with the microphysics in this case, as performance (sensitivity) of the three schemes with prognostic precipitation (M2005, T2009, and MG2) is nearly identical across vertical resolutions. The temporally averaged precipitation rate is similar, but the peak in precipitation rate is higher and earlier at higher vertical resolution. This may indicate that significantly higher vertical resolution is necessary, at least for large updrafts (2 m s^{-1}). However, these rarely occur in the large grid boxes of GCMs.

This work has shown considerable consistency between microphysics schemes designed for global models when tested for idealized cases with a specified flow field or condensation rate and fixed N_c and N_i. This is true primarily for warm rain processes in the three schemes with prognostic precipitation (MG2, M2005, and T2009), while there are larger differences for the ice phase for the M3 and I1 cases. The initiation of rain processes may vary, but the time step and vertical resolution sensitivity of LWP and rain rate are quite similar. On the other hand, MG1.5 with diagnostic precipitation is very different compared to the other three schemes. Major differences in cloud properties between MG1.5 and MG2 are likely for precipitating regimes.

The new scheme (MG2) produces an expected response to cloud droplet number perturbations in the absence of microphysics–dynamics feedbacks. Precipitation is reduced and cloud mass increases with

increasing cloud droplet number concentration, largely by a reduction in the number-dependent autoconversion. Mixed phase clouds are more complicated. Changes in ice number significantly alter ice mass, and this also strongly affects liquid mass, with much larger mass changes in liquid than ice, but about the same relative changes induced by different crystal numbers. This highlights the challenge of representing mixed phase processes in microphysical schemes. Ice mass is dependent on ice nucleation, as well as drop concentration, among other cloud properties.

Finally, the relationship between key process rates in MG2 and MG1.5 is different. MG2 has more precipitation. The precipitation efficiency generally changes less with number concentration than MG1.5 (PE in MG2 is higher for a given drop number concentration). The relationships between autoconversion and accretion are substantially different between MG1.5 and MG2. As expected, addition of prognostic precipitation increases accretion and decreases autoconversion. Accretion increases strongly relative to autoconversion as well with LWP, similar to the findings of Posselt and Lohmann (2009).

These relationships hint that the sensitivity of the MG2 scheme may be lower than MG1.5 to perturbations in cloud droplet number (e.g., by changing aerosol loading), particularly for low drop concentrations ($N_c < 100\,\mathrm{cm}^{-3}$). The relationship of precipitation efficiency and mean LWP with number concentrations are consistent with this result. We examine the impact on model physics in single column and global frameworks in Part II of this work.

Acknowledgments. This work was partially supported by NASA NNX09AJ05G, U.S. DOE ASR DE-SC0006702, and U.S. DOE ASR DE-SC0005336, sub-awarded through NASA NNX12AH90G. The work was also supported by the NSF Science and Technology Center for Multiscale Modeling of Atmospheric Processes (CMMAP), managed by Colorado State University under cooperative agreement ATM-0425247. Thanks to B. Shipway and A. Hill for assistance with the KiD model. Thanks to T. Eidhammer and C. C. Chen for comments.

REFERENCES

Abdul-Razzak, H., and S. J. Ghan, 2000: A parameterization of aerosol activation. 2. Multiple aerosol types. *J. Geophys. Res.,* **105,** 6837–6844, doi:10.1029/1999JD901161.

Bogenschutz, P. A., A. Gettelman, H. Morrison, V. E. Larson, D. P. Schanen, N. R. Meyer, and C. Craig, 2012: Unified parameterization of the planetary boundary layer and shallow convection with a higher-order turbulence closure in the Community Atmosphere Model: Single-column experiments. *Geosci. Model Dev.,* **5,** 1407–1423, doi:10.5194/gmd-5-1407-2012.

Boucher, O., and U. Lohmann, 1995: The sulfate–CCN–cloud albedo effect: A sensitivity study with two general circulation models. *Tellus,* **47B,** 281–300, doi:10.1034/j.1600-0889.47.issue3.1.x.

Cooper, W. A., 1986: Ice initiation in natural clouds. *Precipitation Enhancement—A Scientific Challenge, Meteor. Monogr.,* No. 43, Amer. Meteor. Soc., 29–32, doi:10.1175/0065-9401-21.43.29.

Flatau, P. J., R. L. Walko, and W. R. Cotton, 1992: Polynomial fits to saturation vapor pressure. *J. Appl. Meteor. Climatol.,* **31,** 1507–1513, doi:10.1175/1520-0450(1992)031<1507:PFTSVP>2.0.CO;2.

Fowler, L. D., D. A. Randall, and S. A. Rutledge, 1996: Liquid and ice cloud microphysics in the CSU general circulation model. Part I: Model description and simulated microphysical processes. *J. Climate,* **9,** 489–529, doi:10.1175/1520-0442(1996)009<0489:LAICMI>2.0.CO;2.

Gettelman, A., H. Morrison, and S. J. Ghan, 2008: A new two-moment bulk stratiform cloud microphysics scheme in the NCAR Community Atmosphere Model (CAM3). Part II: Single-column and global results. *J. Climate,* **21,** 3660–3679, doi:10.1175/2008JCLI2116.1.

——, and Coauthors, 2010: Multi-model assessment of the upper troposphere and lower stratosphere: Tropics and trends. *J. Geophys. Res.,* **115,** D00M08, doi:10.1029/2009JD013638.

——, H. Morrison, C. R. Terai, and R. Wood, 2013: Microphysical process rates and global aerosol–cloud interactions. *Atmos. Chem. Phys. Discuss.,* **13,** 11 789–11 825, doi:10.5194/acpd-13-11789-2013.

——, ——, S. Santos, P. Bogenschutz, and P. H. Caldwell, 2014: Advanced two-moment bulk microphysics for global models. Part II: Global model solutions and aerosol–cloud interactions. *J. Climate,* **28,** 1288–1307, doi:10.1175/JCLI-D-14-00103.1.

Ghan, S. J., and R. C. Easter, 1992: Computationally efficient approximations to stratiform cloud microphysics parameterization. *Mon. Wea. Rev.,* **120,** 1572–1582, doi:10.1175/1520-0493(1992)120<1572:CEATSC>2.0.CO;2.

Goff, J. A., and S. Gratch, 1946: Low-pressure properties of water from −160°F to 212°F. *Trans. Amer. Soc. Heat. Vent. Eng.,* **52,** 95–121.

Jiang, H., G. Feingold, and A. Sorooshian, 2010: Effect of aerosol on the susceptibility and efficiency of precipitation in warm trade cumulus clouds. *J. Atmos. Sci.,* **67,** 3526–3540, doi:10.1175/2010JAS3484.1.

Khairoutdinov, M. F., and Y. Kogan, 2000: A new cloud physics parameterization in a large-eddy simulation model of marine stratocumulus. *Mon. Wea. Rev.,* **128,** 229–243, doi:10.1175/1520-0493(2000)128<0229:ANCPPI>2.0.CO;2.

Lebsock, M., H. Morrison, and A. Gettelman, 2013: Microphysical implications of cloud–precipitation covariance derived from satellite remote sensing. *J. Geophys. Res. Atmos.,* **118,** 6521–6533, doi:10.1002/jgrd.50347.

Leonard, B. P., M. K. MacVean, and A. P. Lock, 1992: Positivity-preserving numerical schemes for multidimensional advection. NASA Tech. Memo. NASA-TM-106055, ICOMP-93-05, 62 pp. [Available online at http://ntrs.nasa.gov/search.jsp?R=19930017902.]

Lohmann, U., 2008: Global anthropogenic aerosol effects on convective clouds in ECHAM5-HAM. *Atmos. Chem. Phys.,* **8,** 2115–2131, doi:10.5194/acp-8-2115-2008.

Lopez, P., 2002: Implementation and validation of a new prognostic large-scale cloud and precipitation scheme for climate

and data-assimilation purposes. *Quart. J. Roy. Meteor. Soc.,* **128,** 229–257, doi:10.1256/00359000260498879.

Morrison, H., and A. Gettelman, 2008: A new two-moment bulk stratiform cloud microphysics scheme in the NCAR Community Atmosphere Model (CAM3). Part I: Description and numerical tests. *J. Climate,* **21,** 3642–3659, doi:10.1175/2008JCLI2105.1.

——, J. A. Curry, and V. I. Khvorostyanov, 2005: A new double-moment microphysics parameterization for application in cloud and climate models. Part I: Description. *J. Atmos. Sci.,* **62,** 1665–1677, doi:10.1175/JAS3446.1.

——, G. Thompson, and V. Tatarskii, 2009: Impact of cloud microphysics on the development of trailing stratiform precipitation in a simulated squall line: Comparison of one- and two-moment schemes. *Mon. Wea. Rev.,* **137,** 991–1007, doi:10.1175/2008MWR2556.1.

Posselt, R., and U. Lohmann, 2008: Introduction of prognostic rain in ECHAM5: Design and single column model simulations. *Atmos. Chem. Phys.,* **8,** 2949–2963, doi:10.5194/acp-8-2949-2008.

——, and ——, 2009: Sensitivity of the total anthropogenic aerosol effect to the treatment of rain in a global climate model. *Geophys. Res. Lett.,* **36,** L02805, doi:10.1029/2008GL035796.

Shipway, B. J., and A. A. Hill, 2012: Diagnosis of systematic differences between multiple parametrizations of warm rain microphysics using a kinematic framework. *Quart. J. Roy. Meteor. Soc.,* **138,** 2196–2211, doi:10.1002/qj.1913.

Song, X., G. J. Zhang, and J.-L. F. Li, 2012: Evaluation of microphysics parameterization for convective clouds in the NCAR Community Atmosphere Mode CAM5. *J. Climate,* **25,** 8568–8590, doi:10.1175/JCLI-D-11-00563.1.

Terai, C. R., R. Wood, D. C. Leon, and P. Zuidema, 2012: Does precipitation susceptibility vary with increasing cloud thickness in marine stratocumulus? *Atmos. Chem. Phys.,* **12,** 4567–4583, doi:10.5194/acp-12-4567-2012.

Thompson, G., P. R. Field, R. M. Rasmussen, and W. D. Hall, 2008: Explicit forecasts of winter precipitation using an improved bulk microphysics scheme. Part II: Implementation of a new snow parameterization. *Mon. Wea. Rev.,* **136,** 5095–5115, doi:10.1175/2008MWR2387.1.

Walters, D. N., and Coauthors, 2014: The Met Office Unified Model global atmosphere 4.0 and JULES global land 4.0 configurations. *Geosci. Model Dev.,* **7,** 361–386, doi:10.5194/gmd-7-361-2014.

Wang, M., and Coauthors, 2012: Constraining cloud lifetime effects of aerosols using A-Train satellite observations. *Geophys. Res. Lett.,* **39,** L15709, doi:10.1029/2012GL052204.

Wood, R., T. L. Kubar, and D. L. Hartmann, 2009: Understanding the importance of microphysics and macrophysics for warm rain in marine low clouds. Part II: Heuristic models of rain formation. *J. Atmos. Sci.,* **66,** 2973–2990, doi:10.1175/2009JAS3072.1.